IOSR Journal of Dental and Medical Sciences (IOSR-JDMS)
e-ISSN: 2279-0853, p-ISSN: 2279-0861.Volume 22, Issue 2 Ser.3 (February. 2023), PP 55-63
www.iosrjournals.org

Characterization of liver tissues in CT images using texture analysis

Abdalla Y Mohammed[1], Asma Alamin[1], Mona Ahmed[1],Noha Abdalla[2] and Ahmed Abukonna[1]

[1] *Sudan University of Science and Technology Collage of Medical Radiological Science*
[2] *Khartoum University Faculty of Medicine*

Abstract:
This is an experimental study focuses on the analysis of liver tissues as depicted in CT images using textural features properties to analyze the tissues, it was conducted at the College of Medical Radiologic Sciences in the period from September 2019 to October 2022 after approval of the institutional review board. The data were collected randomly from CT images for abdomen where the liver included in the field of view. The sample includes 60 cases (30 for each class). The liver should represent one of the three classes under the study, the data were taken from male and female, their age should be above 40 and less than 60 years. Diabetic, hypertensive patient and Bilharzias patient were excluded. The data were analyzed using Interactive Data Language (IDL, Version 7.1) as well as Statistical Package for the Social Sciences (SPSS). The data was extracted from each of the images by using a moving window 20×20 pixels where the co-occurrence matrix will be generated and hence Haralick features will be computed using distance one and angle zero. The study found that fifteen textural features were extracted from a number of sub-images (20×20 pixels) represents different liver 'CT' image types were selected from regions that identified by an expert radiologist as fatty, cirrhosis and normal tissue types. The textural features vector was then analyzed by linear regression analysis for selection of the best subset features that can be used to classify the sub-images into their respective class. Eight features were selected as the most discriminant feature; which can be used to classify the images into three classes. The classification coefficient function for fatty liver tissue is as follows: ***Fatty*** *= (entropy × 523.9) + (energy × 30510.5) + (inertia × -0.8) + (IDM × 7.524) + (difference entropy ×-264.9) + (sum variance × 0.6) + (difference variance × 5.6) + (variance of SGLD ×-87.3) -1520.5. The features entropy, energy and IDM is the most discernable fatty liver from the rest of the classes as well as it separate the normal liver from the cirrhotic one. The study concluded that textural features were extracted from selected sub-images that show only the class of interest. The classification technique was adopted as a method of pattern identification of images as three classes. A linear discriminant analysis using stepwise could be used to classify the sample into the predefined classes.*

Keywords: *Fatty liver, CT, Texture analysis.*

Date of Submission: 22-01-2023 Date of Acceptance: 05-02-2023

I. Introduction:

Although the human liver can be imaged with high spatial resolution using X-rays but it is often difficult to interpret. The liver has a complex architecture containing many types of soft tissue. The structure of the liver is varies and the borders between regions of the liver are difficult to assess. Also densities of liver structures are low and there is an overlap between different normal and pathological tissues(1).

CT scanning works very much like other x-ray examinations Due to the nature of planar radiology each pixel of a digitized liver CT scan presents several overlying tissues; with the pixel intensity being determined by the X-ray attenuation through all the different tissue types(2). Often one tissue type dominates attenuation within a pixel and it can be said to represent that particular tissue. Unlike conventional x-rays, CT scanning provides very detailed images CT has been shown to be a cost-effective imaging tool for a wide range of clinical problems(3). CT imaging provides real-time imaging, CT scanning is painless, noninvasive and accurate medical image classification and segmentation is of primary importance in the development of computer assisted diagnosis (CAD) in CT scan systems(4). The identification of normal liver tissues and masses requires highly sophisticated techniques that can isolate regions of interest (ROI) such as fatty liver or cirrhosis liver. The characterization of liver tissues can also facilitate the assessment of normal liver tissues (5).

Although the human liver can be imaged with high spatial resolution using X-rays but it is often difficult to interpret. The liver has a complex architecture containing many types of soft tissue. The structure of

the liver is varies and the borders between regions of the liver are difficult to assess. Also densities of liver structures are low and there is an overlap between different normal and pathological tissues(6).

With the advancement of information technology and hardware, artificial intelligence is now widely employed in a variety of scientific sectors such as medicine, agriculture, construction, tourism, biochemistry, and so on(7). Image processing and computer vision comprise a significant portion of the applications in the various disciplines of artificial intelligence study(8). According to recent study, the human eye recognizes the nature of images using three components: color, texture, and shape. Meanwhile, texture is more significant(9). Image identification and texture analysis are employed in a variety of fields, including medicine(10-12). The aim of this study was to develop a computer programthat allow to characterize fatty liver in CT images.

II. Materials and Methods:

This is an experimental study focuses on the analysis of liver tissues as depicted in CT images using textural features properties to analyze the tissues, it is conducted at the College of Medical Radiologic Sciences in the period from September 2019 to October 2022after approval of the institutional review board. The data were collected randomly from CT scanned for abdomen where the liver included in the field of view. The sample was 60 cases (30 for each class).

The data was extracted from each of the images by using a moving window 20×20 pixels where the co-occurrence matrix will be generated and hence Haralick features will be computed using distance one and angle zero. The textural features were extracted from ROI on the image. A classification technique will be adopted in order to classify the sub-images into three classes. The center of classification will be developed from sub-images that represent the true class according to the advice of an expert radiologist.

Texture features, F_k, can be measured using SGLD matrix derived quantities, known as Haralick's texture features by summing each normalized SGLD matrix element multiplied by a weighting function, $W_k(i, j)$, the function were different for the different features as shown in Table 3-1, generally the features can be calculated as follows:

$$F_k = \sum_{i=0}^{n-1}\sum_{j=0}^{n-1} W_k(i, j) \times p_{d,\theta}(i, j) \qquad \text{Eq. 3-6}$$

Table 3-1 The mathematical description of the SGLD textural features, F_k.

Texture features	**Equation**
Energy (EG)	$EG = \sum_{i=0}^{n-1}\sum_{j=0}^{n-1} p^2(i, j)$ where n is the number of grey levels in the image.
Correlation (CO)	$CO = \dfrac{\sum_{i=0}^{n-1}\sum_{j=0}^{n-1}(i-\mu_x)(j-\mu_y)p(i, j)}{\sigma_x\sigma_y}$ where, $\mu_x = \sum_{i=0}^{n-1} i p_x(i)$, $\sigma_x^2 = \sum_{i=0}^{n-1}(i-\mu_x)^2 p_x(i)$, $\mu_y = \sum_{j=0}^{n-1} j p_y(j)$, $\sigma_y^2 = \sum_{j=0}^{n-1}(i-\mu_y)^2 p_y(j)$, $p_x(i) = \sum_{j=0}^{n-1} p(i, j)$, $p_y(j) = \sum_{i=0}^{n-1} p(i, j)$, are the mean and variance of the marginal distribution $p_x(i)$ and $p_y(j)$.

Results:

The result of this study presented in tables and figures the table's shows the mean and standard deviation of the textural features for the normal, fatty, and cirrhotic liver classes, the confusion matrix of the classification accuracy as well as the classification function co-efficient of the chosen feature that used to classify the liver into the known three classes. The figures include CT images portrayed; normal, fatty and cirrhotic liver as well

as scatter plot of the classification result using the classification function and error plot for each textural feature according to the class types.

Table 2: the mean and Standard deviations of the textural feature for the fatty, cirrhotic and normal liver tissues.

Normal								
statistics	F1	F2	F3	F4	F8	F9	F11	F15
Mean	6.978	0.013	18.436	0.376	2.743	114.642	7.982	5.081
SD	0.886	0.007	29.559	0.107	0.635	119.112	10.872	2.761
Minimum	5.378	0.002	2.342	0.108	1.947	11.451	1.13	1.857
Maximum	9.026	0.035	123.224	0.565	4.463	431.021	45.812	11.489
Fatty								
Statistics	F1	F2	F3	F4	F8	F9	F11	F15
Mean	7.923	0.006	30.553	0.232	3.185	201.244	11.547	7.073
SD	0.884	0.005	32.855	0.068	0.671	141.038	12.988	2.838
Minimum	5.886	0.002	4.382	0.091	2.014	11.887	0.991	2.07
Maximum	9.117	0.02	135.295	0.346	4.533	560.98	54.382	12.156
Cirrhosis								
Statistics	F1	F2	F3	F4	F8	F9	F11	F15
Mean	8.976	0.002	128.823	0.153	4.154	814.471	47.915	15.228
SD	0.404	0.001	95.863	0.095	0.824	212.93	35.923	2.003
Minimum	7.934	0.002	6.342	0.059	2.535	414.733	2.541	10.286
Maximum	9.363	0.006	299.192	0.384	5.059	1308.35	109.454	18.778

Table 3: the classification results versus the ground truth which is scored by a radiologist

	Predicted Group	Predicted Group Membership			
		Normal	Fatty	Cirrhosis	Total
Original	Normal	42	4	0	46
	Fatty	1	65	0	66
	Cirrhosis	2	0	56	58
%	Normal	91.3	8.7	.0	100.0
	Fatty	1.5	98.5	.0	100.0
	Cirrhosis	3.4	.0	96.6	100.0

95.9% classification accuracy of original grouped cases correctly classified.

Table 4 Classification Function Coefficients as calculated by using Fisher's linear discriminant functions

Selected features	Classes		
	Normal	Fatty	Cirrhosis
Entropy	507.8	523.9	511.998
Energy	29803.2	30510.5	30047.854
Inertia	-0.7	-0.8	-0.6
Inverse difference moment	59.3	7.524	37.5

Difference entropy	-247.5	-264.887	-260.6
Sum variance	0.55	0.57	0.56
Difference variance	5.3	5.6	5.1
Variance of SGLD	-84.3	-87.3	-83.2
Constant	-1473.4	-1520.5	-1480.1

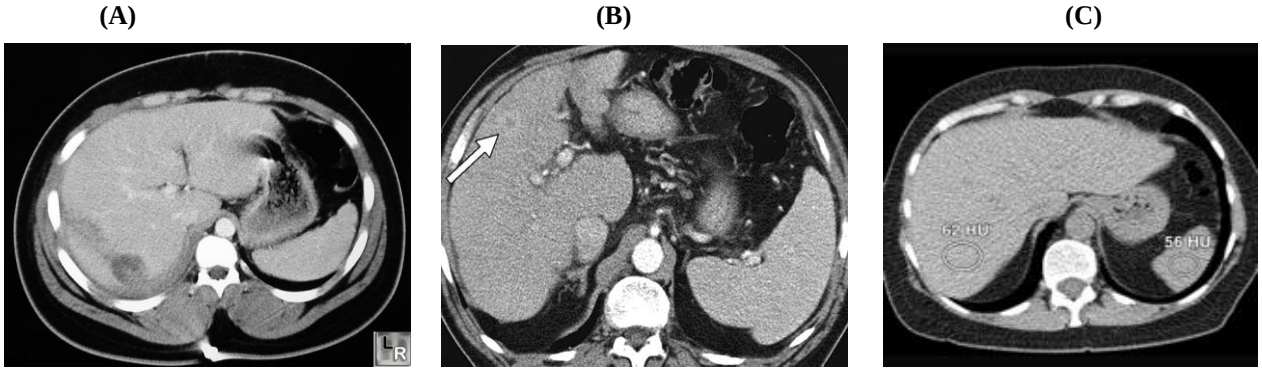

Figure 1: shows three CT images of liver (A) fatty, (B) cirrhosis and (C) normal liver

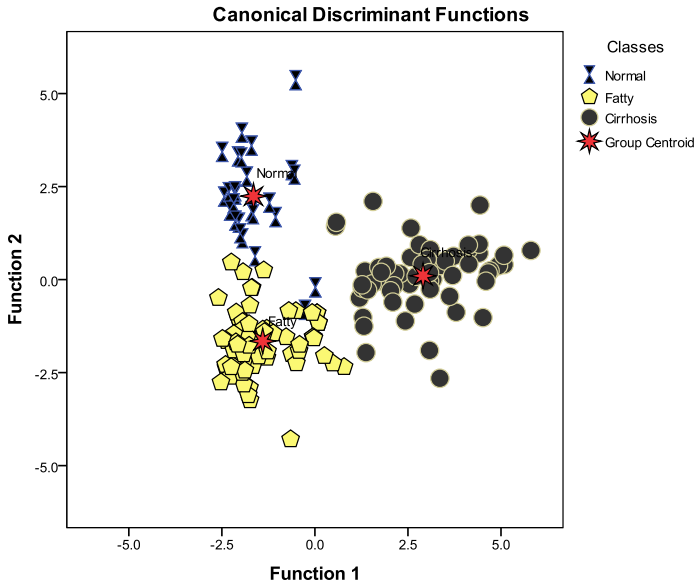

Figure 2: scatter plot of the classified features of the fatty, cirrhosis and normal liver using a classification functions as shown in table 4

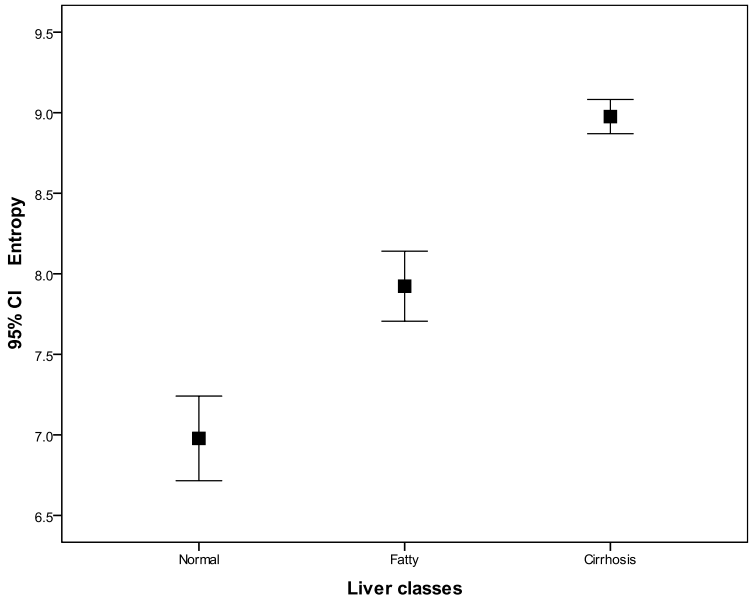

Figure 3 an error bar plot of the entropy features for the fatty, cirrhosis and normal liver tissues with confidence interval of 95%.

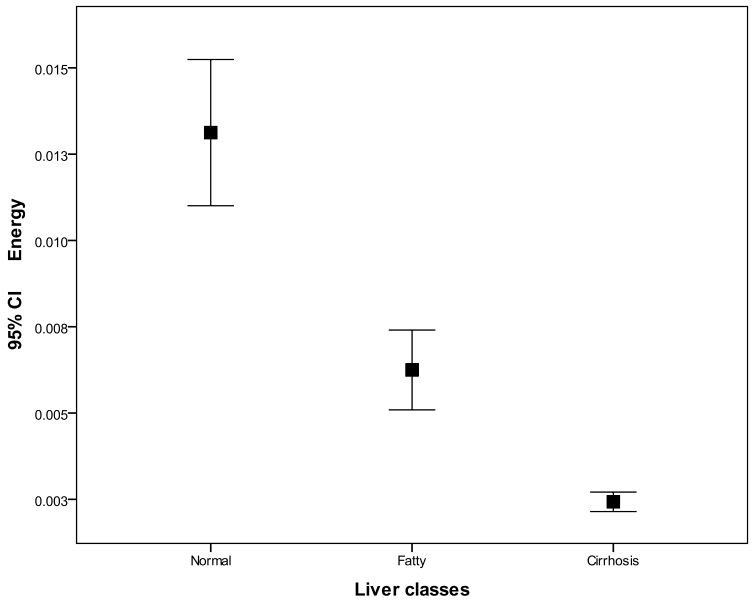

Figure 4: an error bar plot of the energy features for the fatty, cirrhosis and normal liver tissues with confidence interval of 95%.

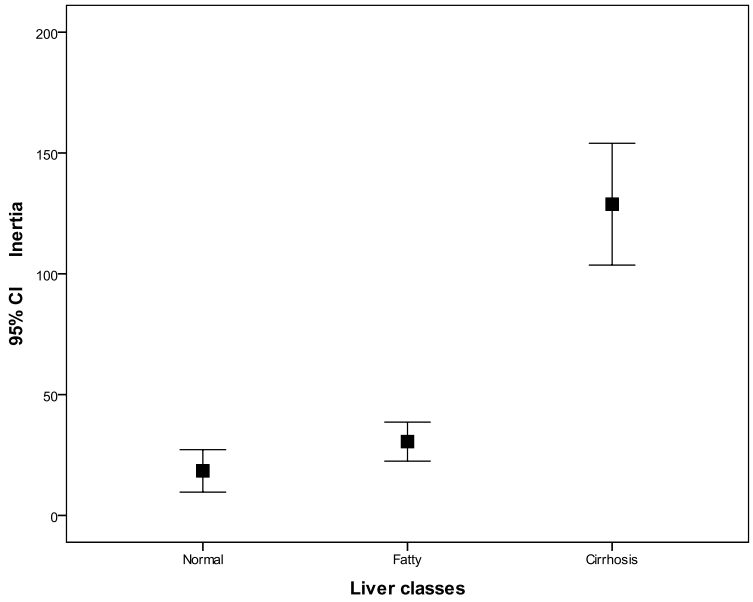

Figure 5 an error bar plot of the inertia features for the fatty, cirrhosis and normal liver tissues with confidence interval of 95%.

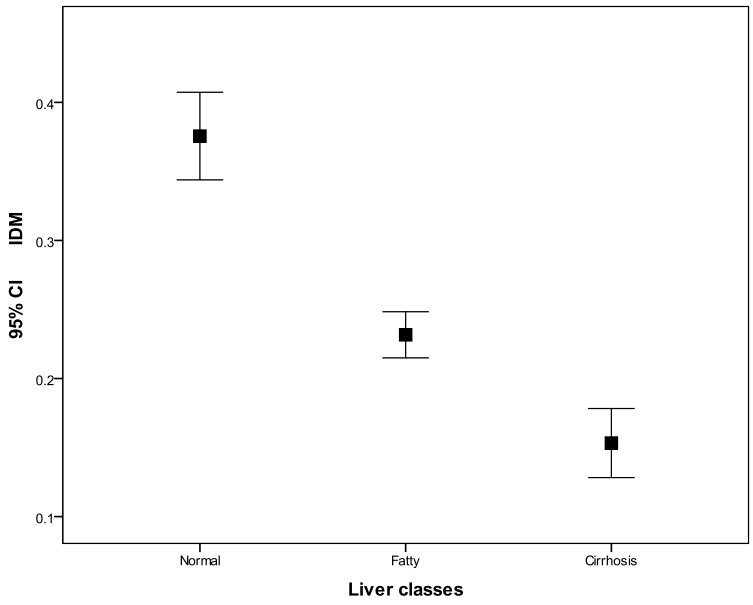

Figure 6: an error bar plot of the inverse different moment features for the fatty, cirrhosis and normal liver tissues with confidence interval of 95%.

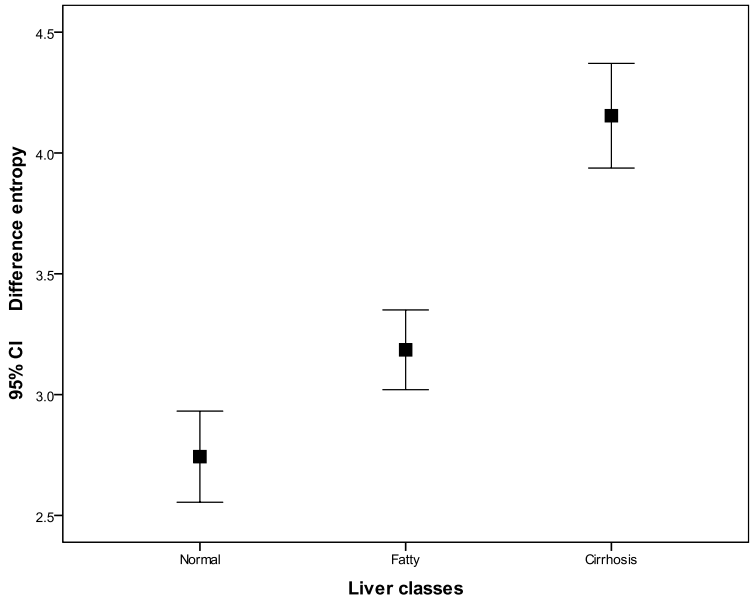

Figure 7: an error bar plot of the difference entropy features for the fatty, cirrhosis and normal liver tissues with confidence interval of 95%.

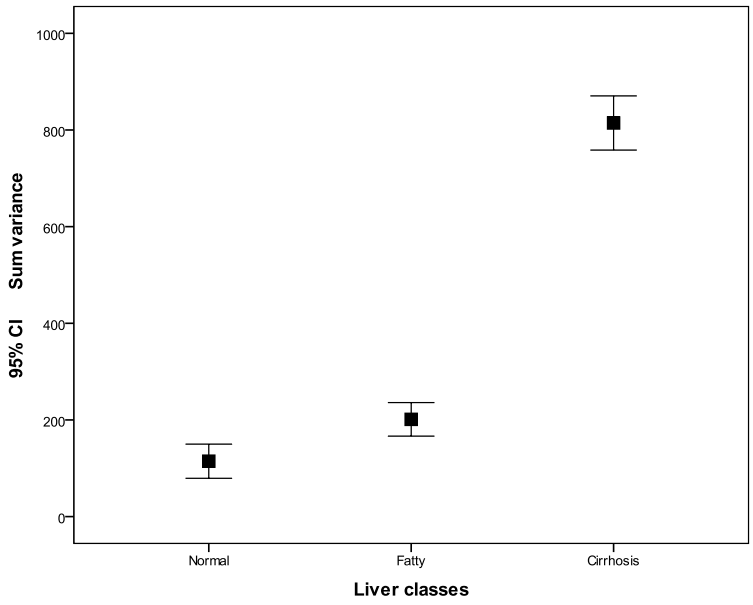

Figure 8: an error bar plot of the sum variance features for the fatty, cirrhosis and normal liver tissues with confidence interval of 95%.

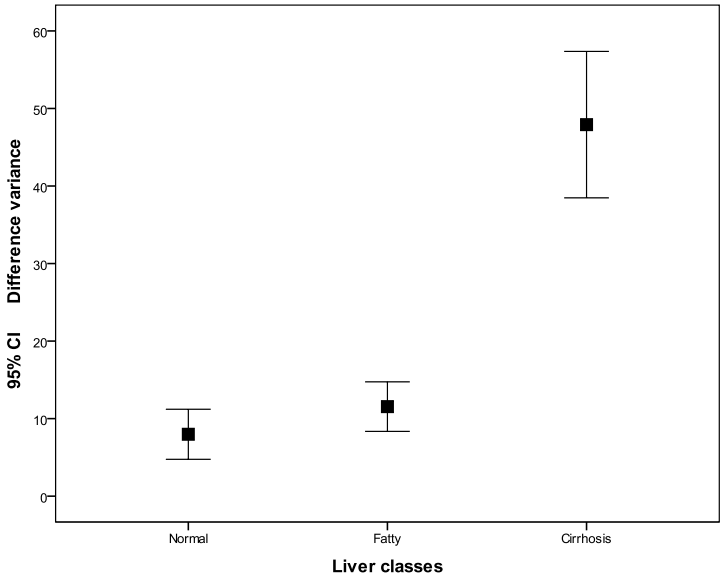

Figure9: an error bar plot of the difference variance features for the fatty, cirrhosis and normal liver tissues with confidence interval of 95%.

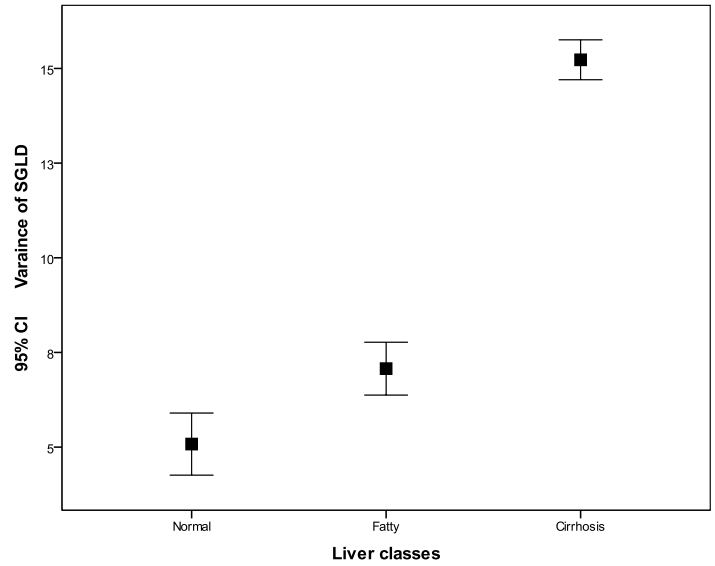

Figure 10: an error bar plot of the SGLD variance features for the fatty, cirrhosis and normal liver tissues with confidence interval of 95%.

III. Discussion:

Fifteen textural features were extracted from a number of sub-images (20×20 pixels) represents different liver 'CT' image types were selected from regions that identified by an expert radiologist as fatty, cirrhosis and normal tissue types. The textural features vector was then analyzed by linear regression analysis for selection of the best subset features that can be used to classify the sub-images into their respective class. Eight features were selected as the most discriminant feature; which can be used to classify the images into three classes. Linear discriminant analysis was applied to classify the features vector into three classes; fatty, cirrhosis and normal liver tissues, using stepwise method. They include: entropy, energy, inertia, inverse difference moment, difference entropy, sum variance, difference variance and variance of SGLD. The classification coefficient function for fatty liver tissue is as follows: Fatty = (entropy × 523.9) + (energy × 30510.5) + (inertia × -0.8) + (IDM × 7.524) + (difference entropy ×-264.9) + (sum variance × 0.6) + (difference variance × 5.6) + (variance of SGLD ×-87.3) -1520.5. The features entropy, energy and IDM is the most discernable fatty liver from the rest of the classes as well as it separate the normal liver from the cirrhotic one (Figure 3, 4 and 5). This means according to the entropy feature the fatty tissue showed a medium or average randomness relative to the other classes similarly the contrast which is depicted by the energy feature and the variations between the fatty

tissues that assembled by the feature IDM; they all revealed average values. Generally the entire selected feature showed that there is a textural difference between fatty and the cirrhotic liver tissues with a minimal overlap between the fatty tissues and the normal liver tissues like in inertia, sum variance, difference variance and SGLD variance; which insure that they represent different pathology. The classification accuracy of fatty tissues was 98.5% while 1.5% of the sub-images that allocated by the expert as fatty were classified by the classifier as normal tissues (Table 2). The classification accuracy of the cirrhotic tissues was 96.6% while 1.5% of the sub-images were classified as normal (Table 2). This result showed that the cirrhotic liver tissues texturally got different representation than the other tissues type (fatty and normal). The textural feature entropy showed a high values with low variation in entropy between the tissues as shown in Figure 3. This means that there is a high randomness' of intensity of pixels occurrence in case of cirrhosis, where the pixels loss their coherence which is mean also there is a considerable amount of heterogeneity in the pixels intensity in respect to neighborhood status. Consequently the cirrhotic tissues showed low values concerning the textural features energy, where the feature energy represents similarity and it is obvious that similarity in case of cirrhosis were compromised 'demolished' (Figure 4). The feature IDM also contribute in the segregation of cirrhosis tissues from fatty and normal since they got high values in respect to liver cirrhosis tissues (Figure 5). In general all features showed a difference between the cirrhotic tissues textures and the other classes. The classification coefficient function for cirrhosis liver tissue is as follows: Cirrhosis = (entropy × 511.9) + (energy ×30047.9) + (inertia ×-0.6) + (IDM × 37.5) + (difference entropy × -260.6) + (sum variance × 0.6) + (difference variance × 5.1) + (variance of SGLD × -83.2) -1480.1.

The normal liver tissues represent wide spectrum of textural values, where definition of normal include wide spectrum of textural properties representation. Generally the eight selected textural feature in the normal liver class showed a considerable amount of variation 'deviation from the mean' as can be noticed in the error bar plots. The feature entropy, energy and inverse different moment (Figure 3, 4 and 5 respectively) separate the normal liver features the fatty and the cirrhosis classes as mention earlier. This situation makes it possible for the classifier to identify the normal liver tissue features form the other classes with accuracy of 91.3% and 8.7% classified as fatty tissues, using a classification score function as follows:

Normal = (entropy × 507.8) + (energy × 29803.2) + (inertia × -0.7) + (IDM × 59.3) + (difference entropy × -247.5) + (sum variance × 0.6) + (difference variance × 5.3) + (variance of SGLD × -84.3) - 1473.4.

The total classification accuracy was 95.9% (Table 2) as portrayed in Figure 4, which is considered reasonable results; since the error in classification might be attributed to the way that the ground truth was scored. The viewer generally identify the whole liver as fatty, cirrhosis or normal liver tissues, indeed part of the tissues might depict normal tissue type or otherwise and this type of tissue cannot be identified or perceived visually by the observer due to their scale of occurrences while it is easier for the texture program to code them as belonging to their original class.

IV. Conclusion:

The study concluded that textural features were extracted from selected sub-images that show only the class of interest. The classification technique was adopted as a method of pattern identification of images as three classes. A linear discriminant analysis using stepwise could be used to classify the sample into the predefined classes.

References:

[1]. Bismuth H. Revisiting liver anatomy and terminology of hepatectomies. Annals of surgery. 2013;257(3):383-6.
[2]. McCollough CH, Leng S, Yu L, Fletcher JG. Dual-and multi-energy CT: principles, technical approaches, and clinical applications. Radiology. 2015;276(3):637-53.
[3]. Higaki T, Nakamura Y, Zhou J, Yu Z, Nemoto T, Tatsugami F, et al. Deep learning reconstruction at CT: phantom study of the image characteristics. Academic radiology. 2020;27(1):82-7.
[4]. Gillies RJ, Kinahan PE, Hricak H. Radiomics: images are more than pictures, they are data. Radiology. 2016;278(2):563-77.
[5]. Gunasundari S, Janakiraman S. A study of textural analysis methods for the diagnosis of liver diseases from abdominal computed tomography. International Journal of Computer Applications. 2013;74(11).
[6]. Kumar S, Moni R, Rajeesh J. An automatic computer-aided diagnosis system for liver tumours on computed tomography images. Computers & Electrical Engineering. 2013;39(5):1516-26.
[7]. Kiani F. Texture features in medical image analysis: a survey. arXiv preprint arXiv:220802046. 2022.
[8]. Dong C-Z, Catbas FN. A review of computer vision–based structural health monitoring at local and global levels. Structural Health Monitoring. 2021;20(2):692-743.
[9]. Armi L, Fekri-Ershad S. Texture image analysis and texture classification methods-A review. arXiv preprint arXiv:190406554. 2019.
[10]. Ponraj N, Mercy M, editors. Texture analysis of mammogram for the detection of breast cancer using LBP and LGP: A comparison. 2016 eighth international conference on advanced computing (ICoAC); 2017: IEEE.
[11]. Fekri-Ershad S, Ramakrishnan S. Cervical cancer diagnosis based on modified uniform local ternary patterns and feed forward multilayer network optimized by genetic algorithm. Computers in Biology and Medicine. 2022;144:105392.
[12]. Althubiti SA, Paul S, Mohanty R, Mohanty SN, Alenezi F, Polat K. Ensemble learning framework with GLCM texture extraction for early detection of lung cancer on CT images. Computational and Mathematical Methods in Medicine. 2022;2022.